

*Ames*

**NASA  
Technical  
Paper  
2614**

August 1986

Trajectory Characteristics  
and Heating of Hypervelocity  
Projectiles Having Large  
Ballistic Coefficients

Michael E. Tauber

(NASA-TP-2614) TRAJECTORY CHARACTERISTICS  
AND HEATING OF HYPERVELOCITY PROJECTILES  
HAVING LARGE BALLISTIC COEFFICIENTS (NASA)  
21 p CSCL 01A

N88-19412

Unclas  
H1/02 0131750

**NASA**

**NASA  
Technical  
Paper  
2614**

1986

Trajectory Characteristics  
and Heating of Hypervelocity  
Projectiles Having Large  
Ballistic Coefficients

Michael E. Tauber

*Ames Research Center  
Moffett Field, California*

**NASA**

National Aeronautics  
and Space Administration

Scientific and Technical  
Information Branch

## NOMENCLATURE

A	base area of body
B	ballistic parameter, see equation (5)
C	constant, see equation (10a)
$C_D$	drag coefficient
g	acceleration of gravity
h	enthalpy
M	constant, see equation (10a)
m	vehicle mass
N	constant, see equation (10a)
q	heat transfer into the body per unit area
$r_n$	nose radius
t	time
V	flight velocity
y	flight altitude
$\beta$	inverse density scale height of atmosphere
$\gamma$	flightpath angle above local horizontal
$\psi$	mass-addition blockage ratio, see equation (14b)
$\rho$	freestream density
$\bar{\rho}$	freestream density normalized by sea level value
$\zeta$	effective heat of ablation

### Subscripts

max	maximum
o	sea level or initial value
s	stagnation point
t	total
w	wall

PRECEDING PAGE BLANK NOT FILMED

## SUMMARY

A simple, approximate equation describing the velocity-density relationship (or velocity-altitude) has been derived for the flight of large ballistic coefficient projectiles launched at high speeds. The calculations obtained by using the approximate equation compared well with results from numerical integrations of the exact equations of motion. The flightpath equation was used to parametrically calculate maximum body decelerations and stagnation pressures for initial velocities from 2 to 6 km/s. Expressions were derived for the stagnation-point convective heating rates and total heat loads. The stagnation-point heating was parametrically calculated for a nonablating wall and an ablating carbon surface. Although the heating rates were very high, the pulse decayed quickly. The total nose-region heat shield weight was conservatively estimated to be only about 1% of the body mass.

## INTRODUCTION

The problem of determining the motion of a projectile through the atmosphere has been studied by ballisticians for over two centuries. When the initial velocity of a projectile is moderate (less than 1 km/s) and its average density high (the specific gravity around ten) then the aerodynamic drag is usually of secondary importance. For these conditions, the simple zero drag and flat-earth formulation given in elementary texts on mechanics describes the trajectory reasonably well (e.g., ref. 1). However, if the projectile is not dense, and the ballistic coefficient ( $m/C_D A$ ) is not large, air drag becomes important, and the equations of motion cannot be solved in closed form. However, various approximations have been made to obtain closed-form expressions which yield reasonably good results (e.g., Allen's work described in ref. 2). Naturally, the equations of motion can always be integrated numerically for specific cases, but generality is lost and, frequently, physical insight is obscured.

The theoretical problem addressed here is that of a large ballistic coefficient projectile launched from the surface of the Earth at a sufficiently high velocity to retain a significant fraction of its initial speed high in the atmosphere, or upon leaving the atmosphere. The closed-form approximate trajectory expression which is derived will be compared with results from numerical integration of the exact equations of motion. Expressions for the forces and heating of the body are derived and numerical values are presented for some example cases.

## TRAJECTORY ANALYSIS

Summing the forces acting along the flightpath gives the equation of motion for a nonlifting body

$$\frac{m}{dt} \frac{dV}{dt} = - \frac{1}{2} C_D A \rho V^2 - mg \sin \gamma \quad (1a)$$

If the initial velocity is high, the phenomena of primary interest here occur while the aerodynamic drag term is much larger than the gravitational term, therefore

$$\frac{dV}{dt} = - \frac{1}{2} \frac{C_D A}{m} \rho V^2 \quad (1b)$$

The flightpath angle measured above the horizontal is

$$\sin \gamma = \frac{1}{V} \frac{dy}{dt} \quad (2)$$

Assuming an exponential variation of atmospheric density with altitude, where  $\rho_0$  is the initial (or sea level) density gives

$$\rho = \rho_0 e^{-\beta y} \quad (3)$$

Differentiating eq. (3), and substituting into eq. (2), yields

$$dt = - \frac{d\rho}{\beta \rho V \sin \gamma} \quad (4)$$

Combining equation (1b) and equation (4), and assuming that the flightpath angle is approximately constant over that portion of the trajectory of primary interest here, gives

$$\frac{C_D A \rho_0}{2m\beta \sin \gamma_0} \int_1^{\bar{\rho}} d\bar{\rho} = \int_{V_0}^V \frac{dV}{V} \quad (5)$$

where  $\rho$  has been normalized by the sea level density so that

$$\bar{\rho} = \rho / \rho_0$$

Assuming

$$B = \frac{C_D A \rho_0}{2m\beta \sin \gamma_0} = \text{constant}$$

permits ready integration of equation (5), and yields the approximate trajectory equation

$$\frac{V}{V_0} = e^{-B(1-\bar{\rho})} \quad (6)$$

where  $V_0$  is the initial velocity. Expressions can now be derived for such characteristics as the flight times, the deceleration of the body, and the stagnation pressure.

The time of flight can be found by substituting the velocity from equation (6) into equation (4)

$$t = \frac{e^B}{\beta V_0 \sin \gamma_0} \int_{\bar{\rho}}^1 \frac{e^{-B\bar{\rho}}}{\bar{\rho}} d\bar{\rho} \quad (7a)$$

Equation (7a) cannot be integrated in closed form. However, the exponential term can be expanded in a series, which converges well for  $B \leq 1$ . The integration can then be performed term-by-term to give,

$$t = \frac{e^B}{\beta_1 V_0 \sin \gamma_0} \left\{ -\ln \bar{\rho}_1 - B(1 - \bar{\rho}_1) + \frac{B^2}{4} [1 - (\bar{\rho}_1)^2] - \frac{B^3}{18} [1 - (\bar{\rho}_1)^3] + \frac{B^4}{96} [1 - (\bar{\rho}_1)^4] \dots \right\} + \frac{e^B}{\beta_2 V_0 \sin \gamma_0} \left\{ \ln \left( \frac{\bar{\rho}_1}{\bar{\rho}_2} \right) - B(\bar{\rho}_1 - \bar{\rho}_2) + \frac{B^2}{4} [(\bar{\rho}_1)^2 - (\bar{\rho}_2)^2] - \frac{B^3}{18} [(\bar{\rho}_1)^3 - (\bar{\rho}_2)^3] + \frac{B^4}{96} [(\bar{\rho}_1)^4 - (\bar{\rho}_2)^4] \dots \right\} \quad (7b)$$

Note that in the integration leading to equation (7b), two density-inverse scale heights,  $\beta_1$  and  $\beta_2$ , were assumed. The change from  $\beta_1$  to  $\beta_2$  occurred at altitude  $\rho_1$ . From sea level to 11 km altitude, the density-scale height varies linearly, and has an average value of about 9.2 km (ref. 3). At higher altitudes, in the stratosphere, the scale height changes abruptly to about 6.4 km (see fig. 1a). The exact variation of density with altitude is compared in figure 1b with values using a scale height of 9.2 km below 11 km of altitude and a scale height of 6.4 km in the stratosphere. The deceleration is given directly by equation (1b) and is a maximum at the initial condition

$$\left( \frac{dV}{dt} \right)_{\max} = - \frac{C_D A}{2m} \rho_0 V_0^2 \quad (8)$$

The stagnation point pressure at high supersonic speeds is approximately

$$p_s \doteq \rho V^2 \quad (9a)$$

The maximum value again occurs at the initial conditions and is

$$(p_s)_{\max} \doteq \rho_0 V_0^2 \quad (9b)$$

In the following section, expressions for the heating rate of the projectile are derived. The heating rates are then integrated to yield expressions for the total heating load.

### HEATING ANALYSIS

In the absence of boundary-layer mass addition, the heating rate per unit area can be approximately expressed in the form (ref. 4)

$$\frac{dq}{dt} = C\rho^N V^M \quad (10a)$$

where  $N$ ,  $M$ , and  $C$  are constants. Equation (10a) is a good approximation for laminar convection (ref. 4;  $N = 0.5$ ,  $M = 3$ ) and turbulent convection (ref. 5;  $N = 0.8$ ,  $M = 3.7$  for  $V > 4$  km/s and  $M = 3.37$  for  $4$  km/s  $> V > 1.5$  km/s). If  $\rho$ ,  $V$ , and the body nose radius,  $r_n$ , are in mks units, then

$$C = \frac{1.85(10^{-8})}{\sqrt{r_n}} \left(1 - \frac{h_w}{h_t}\right)$$

and  $\dot{q}$  will be in  $W/cm^2$ . Substituting equation (6) into equation (10a) gives

$$\dot{q} = C\rho_o^N (\bar{\rho})^N V_o^M e^{-MB(1-\bar{\rho})} \quad (10b)$$

The maximum heating rate occurs at  $\rho = \rho_o$ , which is  $\bar{\rho} = 1$ , and is

$$(\dot{q})_{\max} = C\rho_o^N V_o^M \quad (10c)$$

The total heat load per unit area is

$$q = C\rho_o^N V_o^M \int_0^t (\bar{\rho})^N e^{-MB(1-\bar{\rho})} dt \quad (11a)$$

Substituting equations (4) and (6) into equation (11a) gives

$$q = \frac{C V_o^{M-1} e^{-B(M-1)}}{\beta \sin \gamma_o} \rho_o^N \int_0^1 (\bar{\rho})^{N-1} e^{B(M-1)\bar{\rho}} d\bar{\rho} \quad (11b)$$

Equation (11b) cannot be integrated in closed form. (Note that for  $N < 1$ , the integrand becomes infinite at the lower limit.) However, the exponential term in the integrand can again be expanded in a series, and the integration performed

term-by-term. For  $B(M - 1) \leq 2$ , using the first five terms in the series gives good convergence.

$$q = \frac{C_p N V_o^{M-1} e^{-B(M-1)}}{\beta \sin \gamma_o} \left[ \frac{1}{N} + \frac{B(M-1)}{N+1} + \frac{B^2(M-1)^2}{2(N+2)} + \frac{B^3(M-1)^3}{6(N+3)} + \frac{B^4(M-1)^4}{24(N+4)} + \dots \right] \quad (11c)$$

For the laminar stagnation point without mass addition, the peak heating rate, from equation (10c), is

$$(\dot{q})_{\max} = C \sqrt{\rho_o} V_o^3 \quad (12)$$

while the total heating, from equation (11c), is

$$q = \frac{C \sqrt{\rho_o} V_o^2 e^{-2B}}{\beta \sin \gamma_o} (2 + 1.333B + 0.8B^2 + 0.381B^3 + 0.148B^4 + \dots) \quad (13)$$

Again, note that equation (13) converges well for  $B \leq 1$ .

When mass is added to the boundary layer, such as by forced injection or ablation, equation (10a) must be modified. A well-established approximation is

$$\dot{q} = C_p N V_o^M \psi \quad (14a)$$

where, at the stagnation point (ref. 6)

$$\psi = \frac{1 + 0.72a - [(1 + 0.72a)^2 - 0.52a^2]^{1/2}}{0.26a^2} \quad (14b)$$

and

$$a = \left( \frac{\text{mol. wt. of air}}{\text{mol. wt. of injectant}} \right)^{1/4} \frac{(h_t - h_w)}{\zeta}$$

Here  $\zeta$  is the heat absorbed by the heat-shielding material as it is heated and changes phase. For an ablator,  $\zeta$  is the effective heat of ablation per unit mass. Therefore, the mass of coolant or ablation material required, per unit area, is given by

$$\Delta m = \frac{q}{\zeta} \quad (15a)$$

where the total heat load per unit area now becomes

$$q = C \int \psi \sqrt{\rho} V^3 dt \quad (15b)$$

Heating relations similar to equation (15b) have previously been used successfully to compute the ablation of ballistic-range-launched plastic models at speeds up to 7 km/s (ref. 7).

The above-derived expressions for the trajectory properties and heating will next be applied to a series of example cases for a range of initial velocities.

## RESULTS

### Trajectory Characteristic

The approximate trajectory relation, equation (6), will be compared with computer solutions consisting of the numerical integration of the exact equations of motion using the atmosphere of ref. 3.<sup>1</sup> The body shape is assumed to be cylindrical with a hemispherical nose. For the cases presented, the drag coefficient was essentially constant at a value of 0.92 (ref. 8); the  $m/A$  was assumed to be constant, also. The comparison of equation (6) with results from the exact computation is shown in figure 2 for initial velocities of 3 km/s and 6 km/s, an initial flightpath angle of 45°, and a ballistic parameter  $B = 1$ . Since most of the deceleration occurs at altitudes below 11 km, a scale height of 9.2 km is used. Considering the approximate nature of equation (6), it yields remarkably good results, especially at high speeds. The reason for the decreased accuracy of the approximate equation (6) for the 3 km/s initial-velocity case at altitudes above 20 km is largely caused by assuming a constant flightpath angle. This can be seen in figure 3 where the constant flightpath angle assumption is compared with values from the exact computation. Note that for  $V_0 = 3$  km/s and  $B = 1$ , the apogee of the trajectory is at 45 km, where the flightpath angle becomes zero. If the ballistic coefficient,  $m/C_D A$ , is doubled so that  $B = 0.5$ , however, the flightpath angle change with altitude is much less, being about 20% smaller at 51 km than at the initial value. For the 6 km/s initial velocity case, the constant flightpath angle assumption is seen to be good up to a 60 km altitude, even for  $B = 1$ .

Flight Times- In figure 4, the time to reach altitude as calculated from equation (7b), is compared with the exact computations for initial velocities of 3 and 6 km/s. Equation (7b) is evaluated using  $B = 1$ , a constant flightpath angle of 45°, and scale heights of 9.2 km and 6.4 km. Note the good agreement with the exact computations. The only exception is for  $V_0 = 3$  km at altitudes greater than 20 km where the flightpath angle begins to change significantly.

---

<sup>1</sup>The author thanks his colleague Donn B. Kirk for providing the computer solutions of the exact trajectories.

Maximum Deceleration- The maximum decelerations of two bodies, one with  $B = 0.5$  and the other with  $B = 1$ , are shown in figure 5a as a function of initial velocity. All launches are assumed to occur at sea level. The decelerations are calculated using equation (8), and are essentially identical with the values from the exact computations. Since the peak deceleration occurs at launch, the values are independent of atmospheric variations with altitude. For a ballistic parameter  $B = 1$ , the maximum decelerations range from about 31 g at 2 km/s, to 282 g at 6 km/s. The body with  $B = 0.5$ , has twice as large a ballistic coefficient,  $m/C_D A$ ; therefore, it decelerates less rapidly and experiences only half the peak values of the  $B = 1$  body.

Maximum Stagnation Pressure- The maximum stagnation pressures are shown in figure 5b. The values are computed using equation (9b) and are only a function of the initial velocity and launch altitude. The peak stagnation pressures for sea-level launches are very high, ranging from almost 50 atm at 2 km/s, to nearly 440 atm at 6 km/s. Although the maximum pressures are independent of the ballistic coefficient and the flightpath angle, the rate at which the pressure decreases is a function of these parameters.

The rapid decay of the stagnation pressure is illustrated in figure 6 for initial velocities of 3 and 6 km/s. Note that within 2 sec of a 6 km/s launch, the stagnation pressure decreases to 20% of the peak value, while for the 3 km/s case the pressure falls to about one-third of its peak value. The corresponding altitudes are well below 11 km requiring only the evaluation of the terms in the first bracket, for a single scale height, in equation (7b).

### Heating Environment

The heating rates and total integrated heating at the stagnation point are calculated for two body wall conditions. First, the so-called "cold wall" condition is used where the heating is nearly independent of the state of the wall. Second, a high-density carbonaceous ablator is assumed to protect the nose region of the body, and the heating is influenced by the presence of ablation vapors. A rough estimate of the amount of ablation material required to protect the nose region will be made.

Heating Rates- The variation of the stagnation point heating rate with time is shown in figure 7 for initial velocities of 3 and 6 km/s, for a cold (nonablating) wall. Although the peak heating rates can be very large (nearly 18 kW/cm<sup>2</sup> for the 6 km/s case), note that value declines by nearly an order of magnitude in 3 sec, and that most of the heating occurs within the troposphere below 11 km altitude. The calculations are for  $B = 1$  and a body nose radius of 5 cm.

In figure 8a, the peak heating rates are shown for the same nose radius of 5 cm as a function of initial velocity. Both the cold wall and ablating wall rates are illustrated. A carbon heat shield material having an effective heat of ablation of about 28 MJ/kg was assumed. (The value of 28 MJ/kg is based on the assumption that the ablator sublimates and ignores the effects of surface spallation described in ref. 9. Spallation is likely to occur on these bodies because the surface pressures

are high. However, unlike sublimation, spallation does not reduce surface heat transfer.) The peak heating rate reduction resulting from ablation begins at a speed of about 3.5 km/s and approaches 25% at 6 km/s.

Total Heat Loads- The total time-integrated, stagnation-point heat loads are shown in figure 8b for ballistic parameters of 0.5 and 1 and a constant flightpath angle of 45°. The body with  $B = 1$ , protected by a carbon ablator, experiences total stagnation point heating loads ranging from about 3 KJ/cm<sup>2</sup> at an initial velocity of 2 km/s, to 22 KJ/cm<sup>2</sup> for 6 km/s launches. For the body with  $B = 1$ , the total heating is about 40% less than for the  $B = 0.5$  body since the body with the higher ballistic parameter decelerates more rapidly.

Only modest reductions in total heating result from using a carbon ablator. The largest reduction in total heating occurs for  $B = 0.5$  at the highest speed of 6 km/s and is about 15%. The high effective heat of ablation of carbon results in only a small amount of carbon being vaporized. Therefore, the boundary-layer temperature gradient at the wall is not greatly reduced. However, since the effective heat of ablation is high, only a small amount of heat shield material is ablated. For example, consider the body with  $B = 1$ , launched at 6 km/s and having a hemispherical nose cap of 5 cm radius. If it is assumed that the entire nose cap has a laminar boundary layer, the resultant heating would vaporize only about 62 gm of carbon. While this value could easily increase by several hundred percent owing to spallation and transition to a turbulent boundary layer, the heat shield mass loss would still be modest. (Transition to turbulence is very likely to occur on the nose cap since the local Reynolds numbers are about 4 million at the sonic point (refs. 10 and 11).) It is assumed somewhat arbitrarily, but conservatively, that the total nose-cap heat shield including insulation weighs about ten times the previously calculated mass loss, or about 600 gm. A body consisting of a cylinder with a hemispherical nose, on a 45° flightpath, with  $B = 1$ , would have a mass of about 57 kg. Therefore, the nose-cap heat shield would constitute about 1% of the body's mass. Of course, some heat shielding would also be required on the cylindrical afterbody, but the heating rates there would be much lower than at the stagnation point.

## CONCLUSIONS

A simple, approximate equation describing the velocity-density (or velocity-altitude) relationship has been derived for the flight of large ballistic coefficient projectiles launched at high speeds. Calculations performed using the approximate equation compared well with results from numerical integrations of the exact equations of motion. The flightpath equation was used to parametrically calculate maximum body decelerations and stagnation pressures for initial velocities from 2 to 6 km/s. The peak decelerations ranged up to about 280 g for an initial velocity of 6 km/s, and the peak stagnation pressure was nearly 440 atm. Expressions for the stagnation point convective heating rates and total heat loads were derived. The stagnation point heating was parametrically calculated for a nonablating wall and an

ablating carbon surface. Although the heating rates were very high (nearly 18 KW/cm<sup>2</sup> at 6 km/s for a 5 cm nose radius), the pulse decayed to one-tenth the initial value within 3 sec. For the most severe case calculated, the total stagnation point heat load using a carbon ablator, was 35 KJ/cm<sup>2</sup>. However, the total nose region heatshield mass was conservatively estimated to be only about 1% of the body mass.

Ames Research Center  
Moffett Field, California  
May 2, 1986

## REFERENCES

1. Synge, J. L.; and Griffith, B. A.: *Principles of Mechanics*, McGraw-Hill Book Co. Inc., New York, 1949. 2nd ed.
2. Tauber, M. E.; Kirk, D. B.; and Gault, D. E.: An Analytic Study of Impact Ejecta Trajectories in the Atmosphere of Venus, Mars, and Earth, ICARUS, vol. 33, no. 3, 1978, pp. 529-536.
3. *U.S. Standard Atmosphere, 1962*, U.S. Government Printing Office, Washington, D.C., December 1962.
4. Marvin, J. G.; and Deiwert, G. S.: Convective Heat Transfer in Planetary Gases, NASA TR R-224, July 1965.
5. Arthur, P. D.; Schultz, H. D.; and Guard, F. L.: Flat Plate Turbulent Heat Transfer at Hypervelocities, AIAA Journal of Spacecraft and Rockets, October 1966, pp. 1549-1551.
6. Marvin, J. G.; and Pope, R. B.: Laminar Convective Heating and Ablation in the Mars Atmosphere, AIAA Journal, vol. 5, no. 2, February 1967, pp. 240-248.
7. Wilkins, M. E.; and Tauber, M. E.: Boundary-Layer Transition on Ablating Cones at Speeds up to 7 km/sec, AIAA Journal, August 1966, vol. 4, no. 8, pp. 1344-1348.
8. Hoerner, S. F.: *Fluid-Dynamic Drag, Practical Information on Aerodynamic Drag and Hydrodynamic Resistance*, S. F. Hoerner, Midland Park, N.J., 1958.
9. Lundell, J. H.; and Dickey, R. R.: Ablation of Graphitic Materials in the Sublimation Regime, AIAA Journal, vol. 13, no. 8, August 1975, pp. 1079-1085.
10. Kaattari, G. E.: Effects of Mass Addition on Blunt Body Boundary Layer Transition and Heat Transfer, NASA TP 1139, January 1978.
11. Morkovin, M. V.: Critical Evaluation of Transition from Laminar to Turbulent Shear Layer with Emphasis on Hypersonically Traveling Bodies, AFFDL-TR-68-149, March 1969.

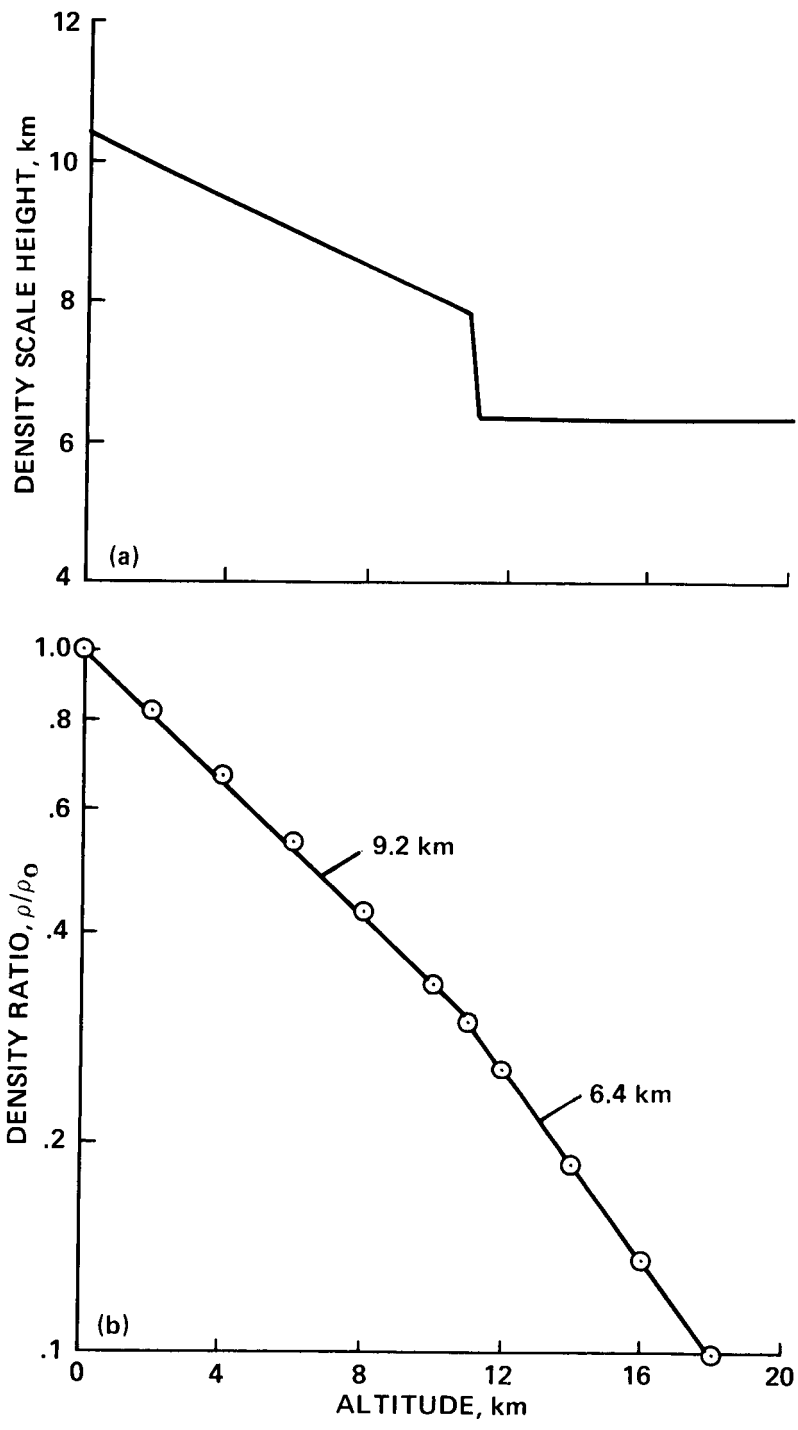


Figure 1.- Atmospheric density variation with altitude.

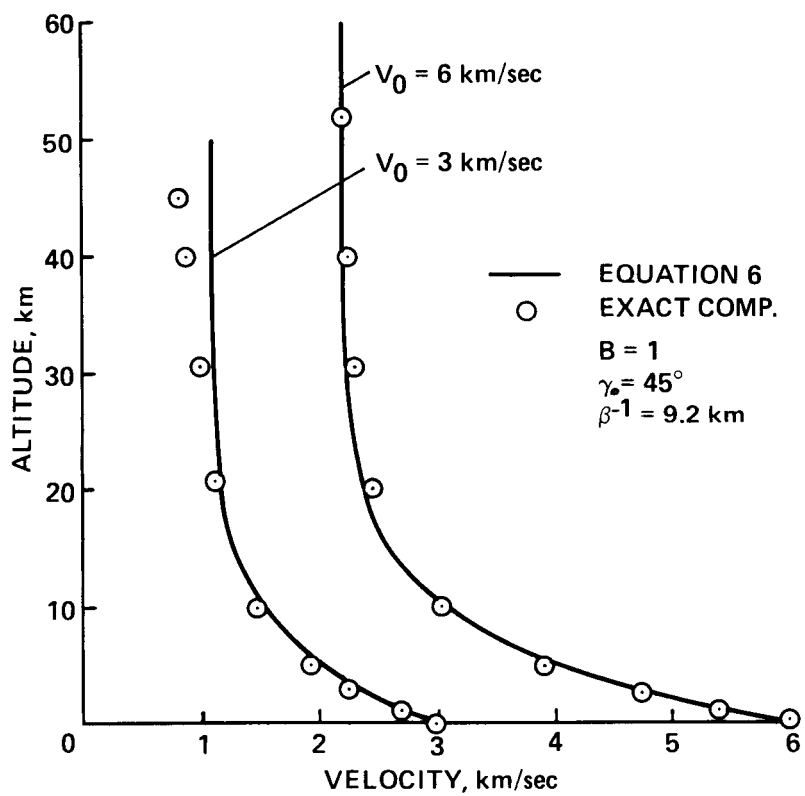


Figure 2.- Comparison of trajectory calculations.

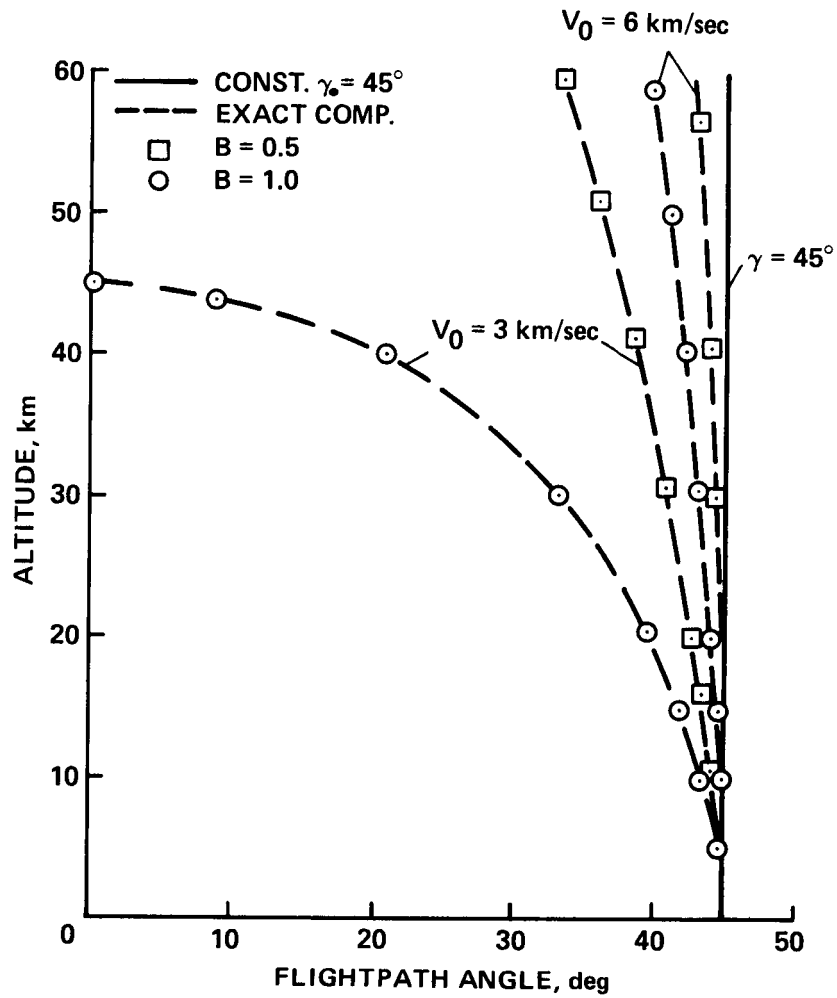


Figure 3.-Flightpath angle comparisons.

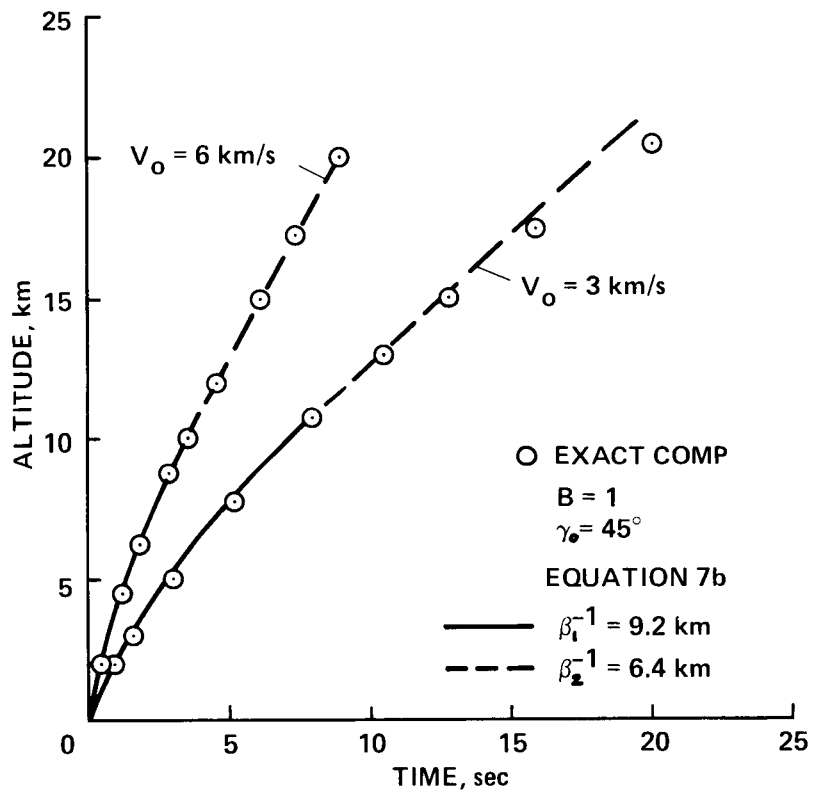


Figure 4.- Flight time calculation comparison.

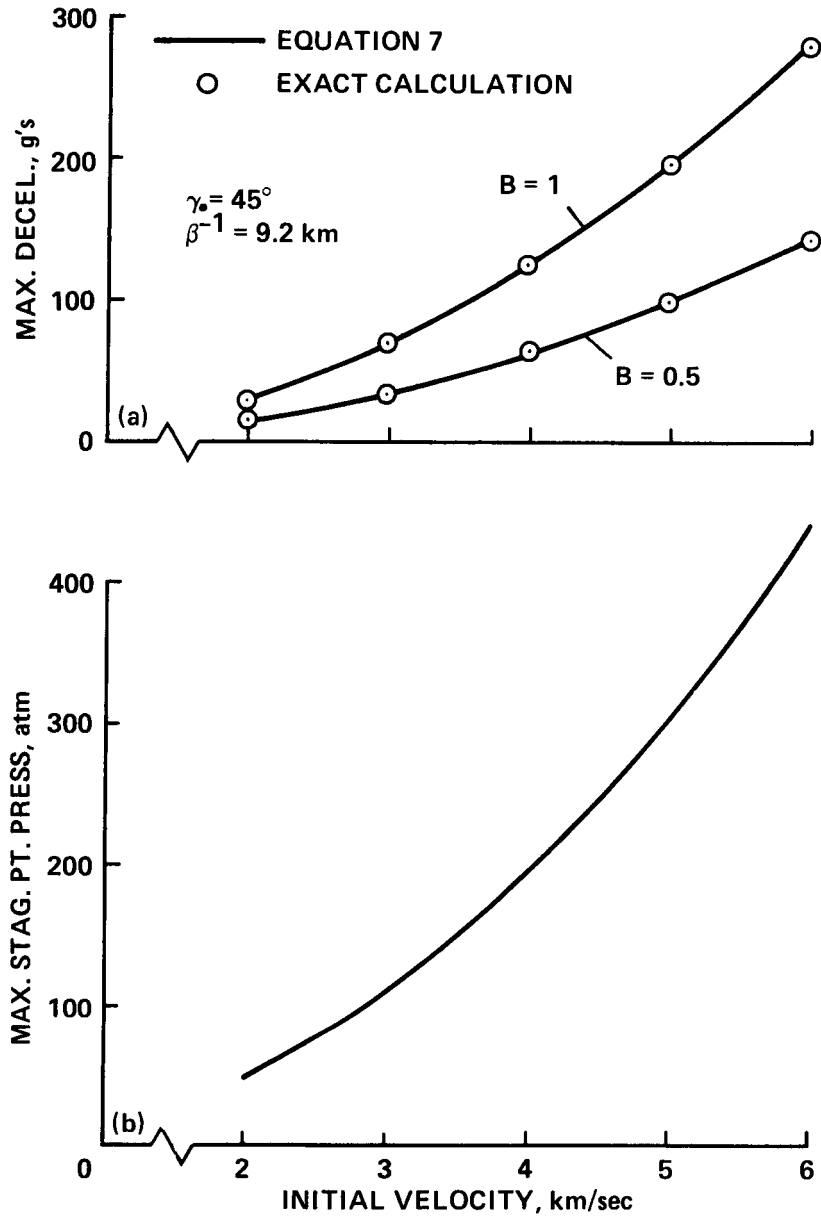


Figure 5.- Maximum decelerations and maximum stagnation pressures encountered.

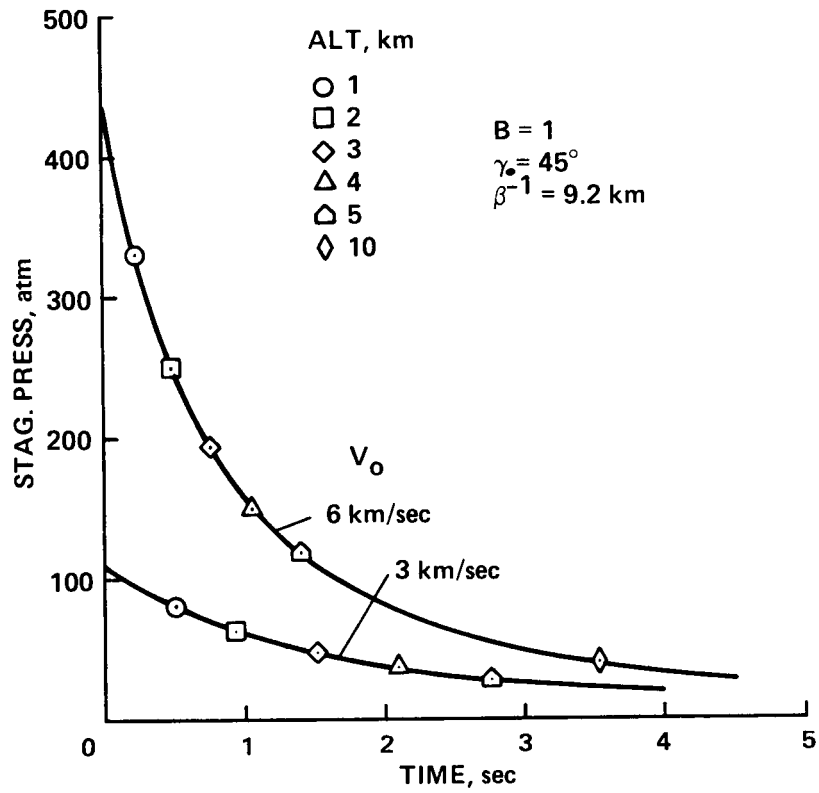


Figure 6.- Stagnation pressure decay.

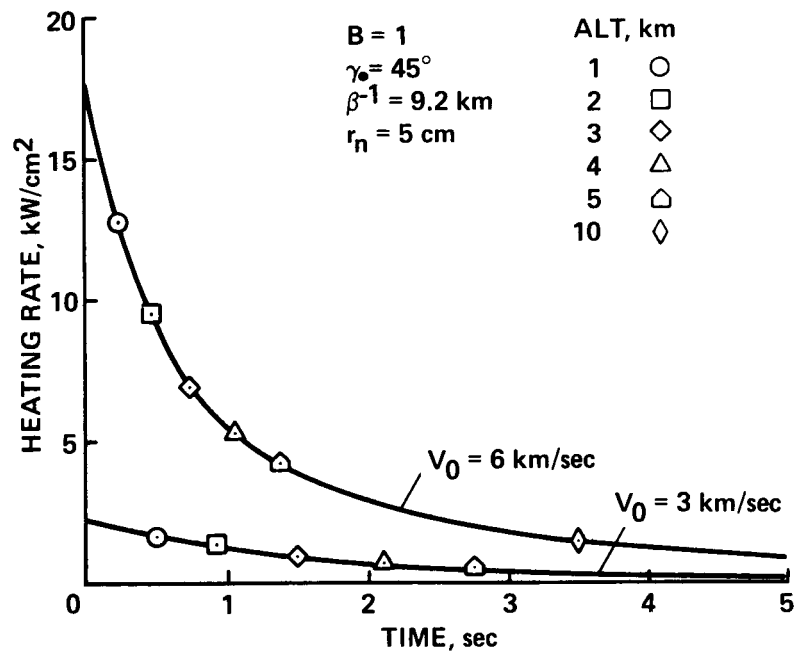


Figure 7.- Stagnation point heating rate decay ("cold" wall).

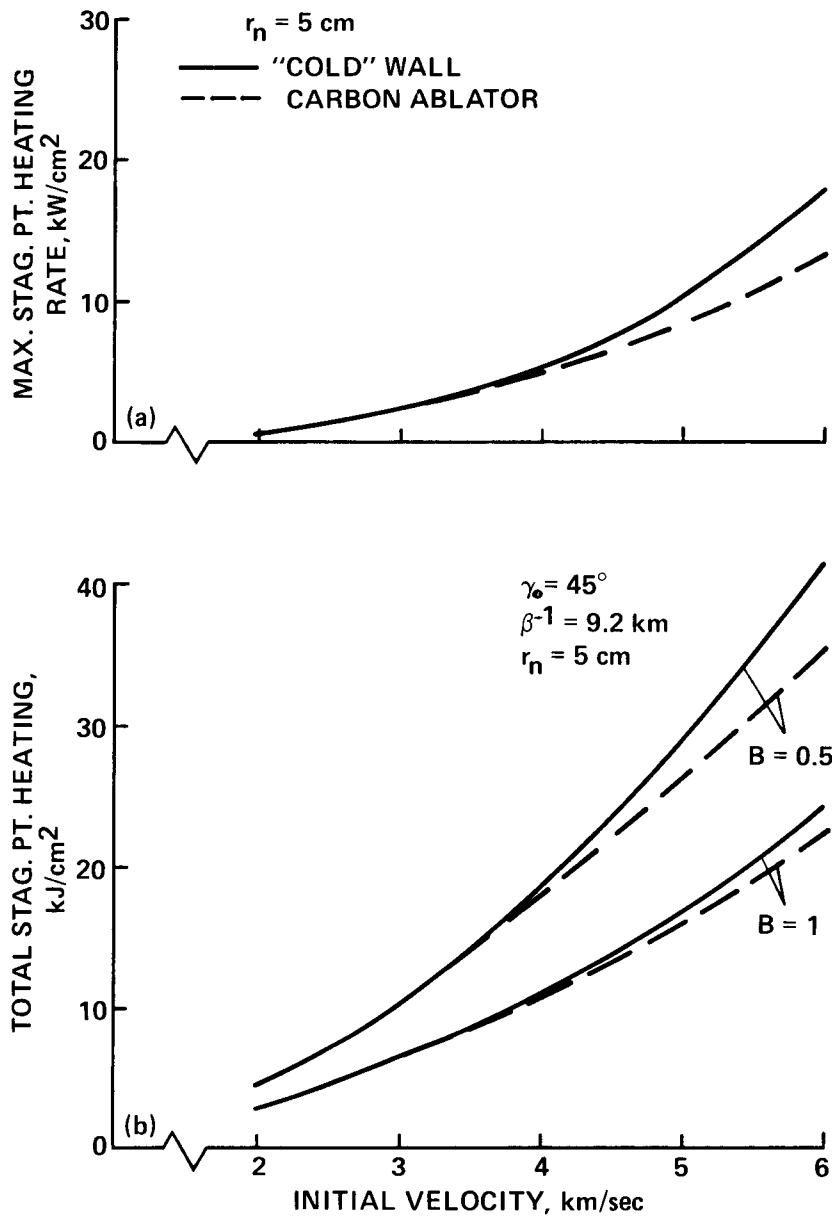


Figure 8.- Maximum stagnation point heating rates and total heating loads encountered.

1. Report No. NASA TP-2614	2. Government Accession No.	3. Recipient's Catalog No.	
4. Title and Subtitle TRAJECTORY CHARACTERISTICS AND HEATING OF HYPERVELOCITY PROJECTILES HAVING LARGE BALLISTIC COEFFICIENTS		5. Report Date August 1986	
		6. Performing Organization Code ATP	
7. Author(s) Michael E. Tauber		8. Performing Organization Report No. A-86187	
		10. Work Unit No.	
9. Performing Organization Name and Address  Ames Research Center Moffett Field, CA 94035		11. Contract or Grant No.	
		13. Type of Report and Period Covered Technical Paper	
12. Sponsoring Agency Name and Address  National Aeronautics and Space Administration Washington, DC 20546		14. Sponsoring Agency Code 506-40-11	
		15. Supplementary Notes Point of contact: Michael E. Tauber, Ames Research Center, MS 230-2, Moffett Field, CA 94035 (415)694-6086 or FTS 464-6086	
16. Abstract  A simple, approximate equation describing the velocity-density relationship (or velocity-altitude) has been derived for the flight of large ballistic coefficient projectiles launched at high speeds. The calculations obtained by using the approximate equation compared well with results from numerical integrations of the exact equations of motion. The flightpath equation was used to parametrically calculate maximum body decelerations and stagnation pressures for initial velocities from 2 to 6 km/s. Expressions were derived for the stagnation-point convective heating rates and total heat loads. The stagnation-point heating was parametrically calculated for a nonablating wall and an ablating carbon surface. Although the heating rates were very high, the pulse decayed quickly. The total nose-region heat shield weight was conservatively estimated to be only about 1% of the body mass.			
17. Key Words (Suggested by Author(s))  Hypervelocity projectile trajectories Aerodynamic heating		18. Distribution Statement  Unclassified - Unlimited  Subject category: 02	
19. Security Classif. (of this report) Unclassified	20. Security Classif. (of this page) Unclassified	21. No. of Pages 21	22. Price* A02

\*For sale by the National Technical Information Service, Springfield, Virginia 22161